Supporting Information

Hong and Dawid 10.1073/pnas.0812880106

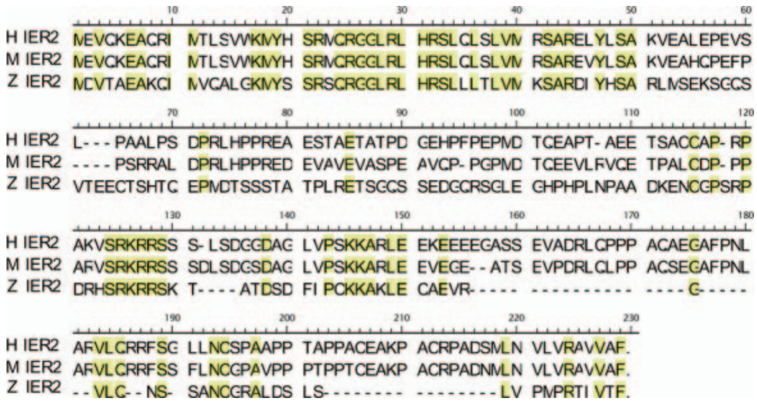

Fig. S1. Vertebrate Ier2 Proteins. Alignment of human, mouse, and zebrafish Ier2 proteins. Amino acid identity is: human vs. zebrafish, 30%; mouse vs. zebrafish, 30%; human vs. mouse 76%. No functional domain was found is Ier2 through computational programs. The accession numbers are: human IER2, NM004907mouse Ier2, NM010499; zebrafish Ier2, EU815060.

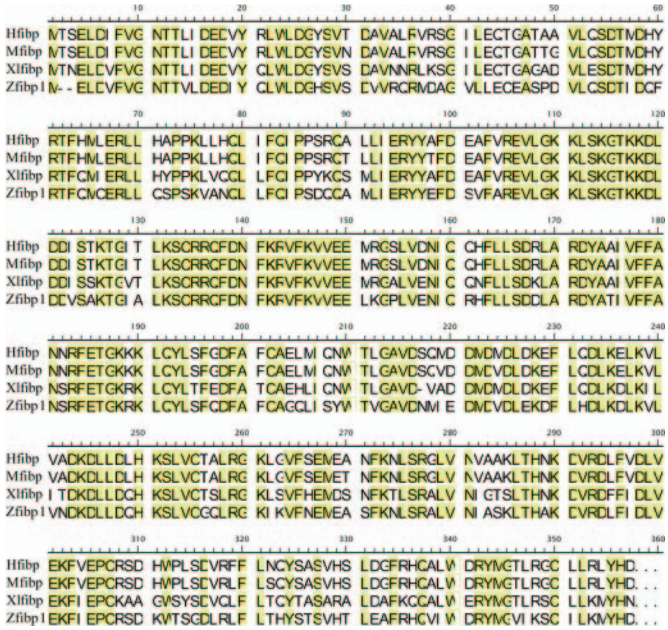

Fig. S2. Alignment of Fibp Amino Acid Sequence. Zebrafish Fibp1 is 70% identical to human, mouse, and *Xenopus* Fibp1, *Xenopus* and human or mouse are 77–78% identical, whereas human and mouse are 97% identical. Computational analysis programs did not reveal functional domains in Fibp1. The accession numbers of Fibp1 family members are: human (AF171946); mouse (NM021438); *Xenopus* (BC097711); zebrafish (BC085535).

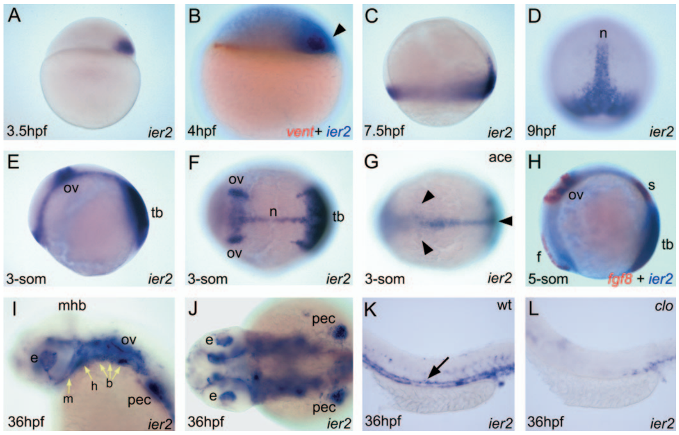

Fig. S3. Expression Pattern of *ier2*. (*A*) Lateral view of *ier2* expression at 3.5hpf. *ier2* expression can be detected only after the midblastula transition (MBT). (*B*) Lateral view of 2-color in situ hybridization of *ier2* (blue) and the ventral marker *vent* (red) at 4hpf. Arrowhead points to *ier2* expression at the dorsal side. (*C*) Lateral view of *ier2* expression at 7.5hpf in the marginal region. (*D*) Dorsal view of notochord and marginal region expression of *ier2* at 9hpf. (*E*–*G*) Lateral (*E*) and dorsal views (*F* and *G*) of *ier2* expression pattern of wt (*E* and *F*) and *ace* (*G*) embryos at the 3-somite stage. Arrowheads in *G* indicate loss of *ier2* expression in *ace* mutant. (*H*) Lateral view of 2-color in situ hybridization of *ier2* (blue) and *fgf8* (red) at the 5-somite stage. (*I*–*L*) Lateral (*I*, *K*, and *L*) and dorsal view (*J*) of *ier2* expression in the head (*I* and *J*) and trunk (*K* and *L*) region at 36hpf. Yellow arrows in *I* indicate pharyngeal expression of *ier2*. Arrow in *K* points to blood vessel. b, brachial arch; e, eye; f, forebrain; h, hyoid arch; m, mandibular arch; n, notochord; ov, otic vesicle; pec, pectoral fin; tb, tail bud.

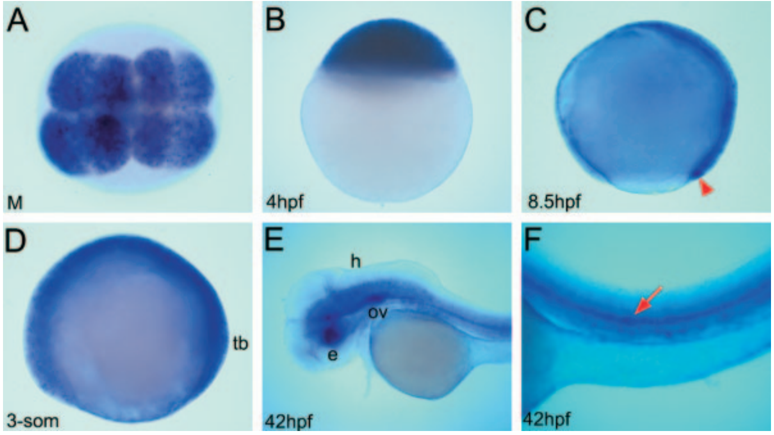

Fig. S4. *fibp1* Expression Pattern. (*A*) Dorsal view of maternal expression of *fibp1* at the 8-cell stage. (*B*) Lateral view of *fibp1* expression at 4hpf. (*C*) Lateral view of *fibp1* expression at 8.5hpf. A red arrowhead points to *fibp1* expression in the fore-runner cells that are precursors of Kupffer's vesicle. (*D*–*F*) Ubiquitous expression of *fibp1* at 3-somite and 42hpf stages (*E* and *F*). Arrow in *F* points to the notochord.

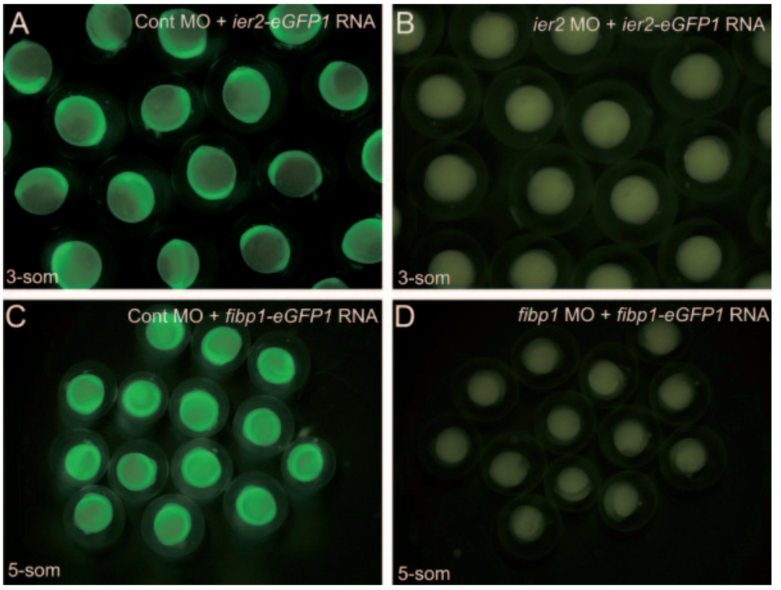

Fig. S5. Efficiency of *ier2* and *fibp1* MOs. (*A* and *B*) *ier2* MO plus *ier2-egfp1* RNA-injected embryos completely lost the GFP signal (*b*) compared with control MO-injected embryos (*a*), as seen at the 3-somite stage. (*C* and *D*) *fibp1* MO likewise inhibited the GFP signal d, as seen at the 5-somite stage.

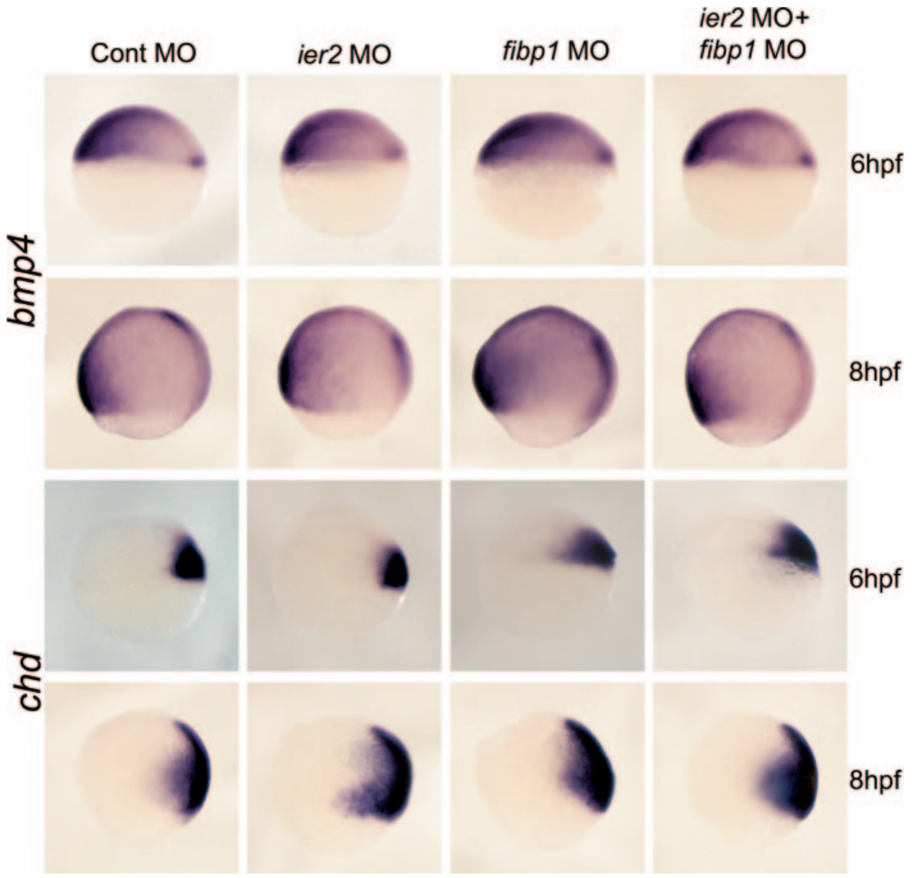

Fig. S6. Dorsal-ventral axis specification in MO injected embryos. Embryos were injected with the MO shown at the top of each column, fixed at the times shown on the right, and hybridized with *bmp4* (ventral marker) or *chordin* (dorsal marker) as indicated on the left. The injection of these MOs had no substantial effect on the dorsal-ventral patterning of these embryos.

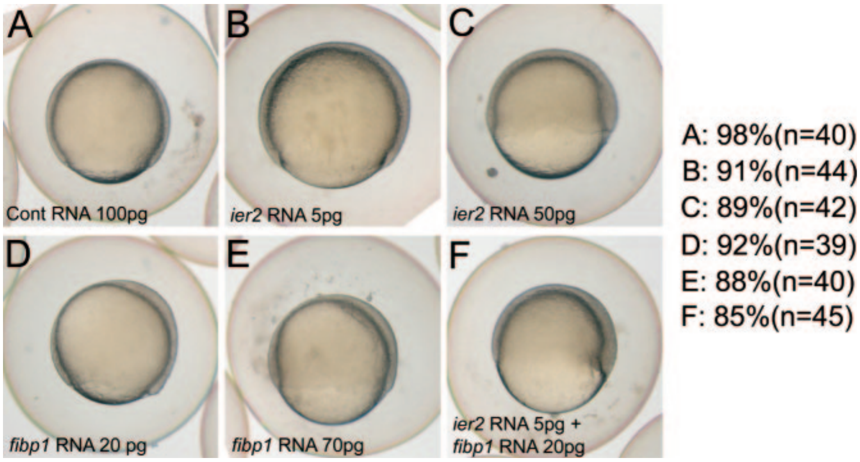

Fig. S7. Synergism between *ier2* and *fibp1* RNA injection. Embryos were injected as indicated in the figure and photographed at the same time when control embryos were at 80% epiboly. A dosage dependent delay in epiboly is seen after RNA injection, with a synergistic effect of injection of both RNA. To the right are shown percentages of embryos for each condition that look like the embryo illustrated–thus the numbers represent normal embryos in *A*, *B*, and *D* and delayed embryos in *C*, *E*, and *F*.